

# PROCEEDINGS OF SPIE

[SPIDigitalLibrary.org/conference-proceedings-of-spie](https://spiedigitallibrary.org/conference-proceedings-of-spie)

## Behavior of GeSbTeBi phase-change optical recording media under sub-nanosecond pulsed laser irradiation

Kazuo Watabe, Pavel Polynkin, Masud Mansuripur

Kazuo Watabe, Pavel Polynkin, Masud Mansuripur, "Behavior of GeSbTeBi phase-change optical recording media under sub-nanosecond pulsed laser irradiation," Proc. SPIE 5380, Optical Data Storage 2004, (9 September 2004); doi: 10.1117/12.557067

**SPIE.**

Event: Optical Data Storage Topical Meeting, 2004, Monterey, California, United States

# \*Behavior of GeSbTeBi phase-change optical recording media under sub-nanosecond pulsed laser irradiation

Kazuo Watabe<sup>\*a</sup>, Pavel Polynkin<sup>b</sup>, Masud Mansuripur<sup>b</sup>

<sup>a</sup>Core Technology Center, Toshiba Corporation  
8, Shinsugita-cho Isogo-ku, Yokohama 235-8522, Japan;

<sup>b</sup>Optical Sciences Center, The University of Arizona  
1630 E. University Blvd., Tucson, AZ 85721, USA

## ABSTRACT

Reflectivity variations during phase-transition between amorphous and crystalline states of a Bi-doped GeTe-Sb<sub>2</sub>Te<sub>3</sub> pseudo-binary compound film is investigated with sub-nanosecond laser pulses using a pump-and-probe technique. We also use a two-laser static tester to estimate the onset time of crystallization under a 2.0- $\mu$ s-pulse excitation. Experimental results indicate that the formation of a melt-quenched amorphous mark is completed in about one nanosecond, but crystalline mark formation on an as-deposited amorphous region requires several hundred nanoseconds. Simple arguments based on heat diffusion are used to explain the time scale of amorphization and the threshold for creation of a burned-out hole on the phase-change film.

**Keywords:** Phase-change recording, crystallization, amorphization, pump and probe technique, sub-nanosecond

## 1. INTRODUCTION

In rewritable optical data storage, phase-change materials have become mainstream in the market place, as is used for rewritable DVDs such as DVD-RAM and DVD-RW. In a phase-change medium, writing and erasing of data bits are performed by controlling the power of irradiating laser pulses focused onto the recording layer of the medium.<sup>1-5</sup> Writing is carried out by creating amorphous marks on an initialized, i.e., crystallized, region of the phase-change medium. Such amorphization is induced by melting followed by rapid cooling of the material. A short, relatively high-power pulse focused on the phase-change film causes its local temperature to reach beyond the melting temperature  $T_m$  of the film, thus causing local melting. Once the pulse has been terminated, the molten pool cools rapidly to form a solid, melt-quenched amorphous mark. Erasing of recorded bits is performed by recrystallizing the amorphous marks. Crystallization is induced by localized annealing. A focused laser beam of moderate power raises the local temperature of the film to its glass transition point  $T_g$  keeps the temperature below  $T_m$ . Maintaining the temperature between  $T_g$  and  $T_m$  for a sufficient period of time reverts the amorphous mark to crystalline state. Optical readout of the information bits thus recorded requires evaluating the reflectivity change caused by an array of amorphous marks on a crystalline background. Usually, the amorphous state has lower reflectivity than the crystalline state. A focused CW laser beam at sufficiently low power does not change the local state of the film, but reproduces the recorded marks by the change in reflectivity, which is ultimately picked up by a photodetector.

In optical data storage, demand for large capacity and high data transfer rate continues to grow. To achieve a high data rate, one must write data bits (i.e., marks and spaces) in a short time interval, which means that amorphous marks must be formed by short laser pulses. Moreover, direct overwrite of previously recorded marks requires rapid recrystallization as well. Modern optical data storage relies on laser pulses on the order of 10 ns duration, obtained by direct modulation of semiconductor diode lasers. It thus seems natural to investigate pulses on the order of nanosecond or sub-nanosecond duration to achieve high data transfer rates in future optical storage devices.

The experimental studies of Afonso *et al* highlighted reversible amorphization and crystallization of phase-change materials under femtosecond and picosecond laser pulses,<sup>6,7</sup> thus affirming the tremendous potential of this class of materials for high-speed rewritable optical data storage applications. At this point, however, there are practical

---

\* kazuo.watabe@toshiba.co.jp

obstacles to implementing femtosecond or picosecond lasers in a viable commercial storage unit. Nevertheless, we remain interested in phase-change phenomena brought about with sub-nanosecond (i.e., on the order of 0.1 ns) laser pulses, which may be practical for the next generation of rewritable optical data storage products.

In this paper we investigate the transition between amorphous and crystalline phases of a phase-change material induced by a 0.5-ns pulsed laser. A pump-and-probe technique is used to monitor the reflectivity variation in phase-change events,<sup>8,9</sup> starting just before the onset of the 0.5-ns pulse and continuing throughout and after the end of the pulse. We used quadrilayer samples containing on a phase-change film of GeTe-Sb<sub>2</sub>Te<sub>3</sub> pseudo-binary composition in which a few percent of Sb is replaced with Bi.<sup>10</sup>

## 2. EXPERIMENTAL SET UP

The experimental set up is shown schematically in Fig. 1. The details of the construction and functioning of the tester are given elsewhere.<sup>8,9</sup> A Q-switched solid-state laser ( $\lambda = 532\text{nm}$ ) is used as the light source. The laser emits a train of pulses, whose duration is 0.5ns long and repetition rate is 5.7kHz. We pick a single pulse out of this train with an acousto-optic (AO) modulator, which acts as an optical gate. A single pulse is then divided into a pump beam and a probe beam. The probe beam is set to have much weaker intensity, about a factor of 40 less than the pump beam, so that it won't affect the phase transition of the sample. We adjust the time delay between the pump and probe pulses by changing the optical path length of the pump beam, which is simply done by adjusting the position of a retroreflector in its path. The pump and probe beams are recombined at the second PBS and irradiated onto the sample through a microscope objective. In this research, we used a 0.4-NA objective lens. The probe coincided at the sample with the pump beam; thus the probe picks up its signal from the central portion of the mark formed by the pump beam, though the reflected signal will be affected by the surroundings of the mark due to the spatial distribution of the focused probe beam at the sample. The signal from the probe is averaged over 20 runs, where each run is performed on a fresh point of the sample. (The position of the sample is shifted by  $2.5\ \mu\text{m}$  for each run.)

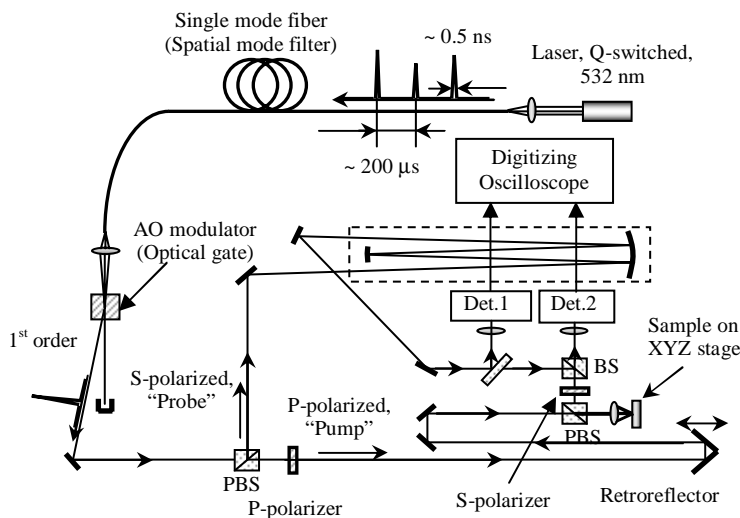


Fig. 1. Experimental set-up of the pump-and-probe tester

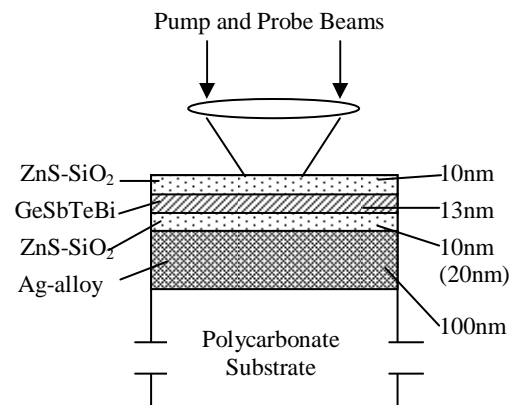


Fig. 2. Structure of the quadrilayer phase-change optical storage medium used in this research

The samples used in this study had a typical quadrilayer structure for front-surface access, where the 0.6-mm-thick substrate is directly beneath the metal (reflective) layer. Figure 2 shows the cross-sectional view of the sample. The stack consists of a 10-nm-thick ZnS-SiO<sub>2</sub> upper dielectric layer, a 13-nm-thick GeSbTeBi phase-change recording layer, a 10-nm-thick (20-nm-thick) ZnS-SiO<sub>2</sub> lower dielectric layer and a 100-nm-thick silver alloy reflective layer. We hereafter call the sample with a 10-nm-thick lower dielectric layer Disc A and the sample with a 20-nm-thick lower

dielectric layer Disc B. The silver alloy layer acts as a reflector and also as a heat sink, which removes the heat from the phase-change layer deposited there by the laser. Thus, we use two kinds of samples that have different thicknesses of the lower dielectric layer to compare their thermal characteristics. We focused the pulsed laser beam through the upper dielectric layer, and not through the substrate, in order to avoid the influence of the birefringence of the substrate, which can cause a coherent pump-and-probe crosstalk at the signal detector.<sup>9</sup>

The phase-change film in our samples had the GeTe-Sb<sub>2</sub>Te<sub>3</sub> pseudo-binary composition, with a few percent of Sb replaced by Bi to help the crystallization process by reducing the threshold temperature for crystallization.<sup>10</sup> (This material will be referred to as GSTB film hereafter). As a result, the recording layer has four elements, namely Ge, Sb, Te and Bi. This type of phase-change film is believed to have a crystallization process that is dominated by growth of nuclei.

We measured the reflectivity for three different states of the phase-change sample. These are the as-deposited (amorphous) state, the crystalline state, and the melt-quenched amorphous state. The crystalline state is obtained by annealing a fairly large as-deposited region of the sample at a moderate temperature. Here, we use a static tester<sup>11,12</sup> to anneal the sample in the as-deposited state by scanning it with a focused cw laser beam at a few milliwatts of power. The melt-quenched amorphous state is obtained by irradiating a previously initialized, i.e., crystallized, area of the sample with a 0.5 ns pulse. We wrote an array of closely spaced melt-quenched amorphous marks on a crystalline region of the samples by 0.5-ns pulses at 0.25 nJ per pulse. It is conventionally believed that writing amorphous marks so close to each other does not necessarily create a pure melt-quenched amorphous region on phase-change samples. This is because writing amorphous marks typically creates a crystalline ring around the circular amorphous mark during cool-down where the ring region spends sufficient time in the temperature range between  $T_g$  and  $T_m$ . In our experiment, however, due to the short duration of the pulse the melt-quenched amorphous marks do not have this crystalline ring around them. We thus create a fairly large melt-quenched amorphous region on our phase-change samples.

Table 1. Reflectivities of the three states of the phase-change samples at  $\lambda = 532$  nm.

	Disc A	Disc B
Crystalline area	35.4%	30.8%
As-deposited amorphous area	8.09%	14.51%
Melt-quenched amorphous area	9.26%	14.86%

The measured reflectivities of the various states for our two samples are listed in Table 1. The reflectivity of the melt-quenched amorphous state is found to be slightly higher than that of the as-deposited state for both discs, which agrees with results reported in the literature.<sup>13,14</sup> Melting and subsequent cooling of a phase-change material can create small crystallites, or crystalline embryos, as the temperature of the film passes through the range between  $T_g$  and  $T_m$ .<sup>15,16</sup> These embryos raise the reflectivity of the melt-quenched amorphous state slightly above that of the as-deposited state, which presumably does not have any such crystalline embryos.

### 3. EXPERIMENTS ON CRYSTALLINE FILM

Localized amorphization of the crystalline state of the storage layer corresponds to writing marks on a phase-change optical disc, which is usually initialized to the crystalline state in advance. Figure 3 shows the measured reflectivity change during crystalline-to-amorphous phase-change of the GSTB film of Disc A. After writing on this sample by short pulses, we bring it to a static tester<sup>11,12</sup> and try to erase (i.e., recrystallize) the marks by a focused cw laser beam to confirm the state of the marks. Figure 4 shows microscope images of the written marks; the pictures in the right-hand side (b) show the marks after erasure. This observation confirms that the bottom curve (corresponding to 0.53 nJ) in Fig. 3 represents the formation of a permanent hole in the film rather than a melt-quenched amorphous mark (see Fig. 4, lower). Marks written at 0.16nJ are hardly discernible from the crystalline background under an optical microscope, even though at least a tiny mark is expected to have formed according to Fig. 3 by the slight drop in the reflectivity of the sample. The two curves in the middle of Fig. 3 illustrate the formation of distinguishable melt-quenched amorphous marks. In these cases, the reflectivity drops right after the beginning of the pulse ( $t = 0.0$  ns) and reaches its lowest value

at the end of the pulse ( $t = 0.5$  ns). After reaching minimum, the reflectivity goes up ever so slightly for several hundred picoseconds before reaching its final value; this corresponds to the cooling and solidification process. If we suppose that the thermal conductivity  $K$  and the specific heat  $C$  of the GSTB film and dielectric layers are nearly the same as inferred from other sources ( $K=0.005$  J/cm/s $^{\circ}$ C,  $C=1.5$  J/cm $^3$ / $^{\circ}$ C),<sup>15</sup> we can estimate how far the heat flows during laser exposure. In a time  $t$ , heat diffuses a typical distance  $L = (Kt/C)^{1/2}$ , which, for  $t = 0.5$  ns, yields a value for  $L$  around 13 nm.<sup>17</sup> Thus right after the 0.5 ns duration of the pulse, the heat can reach the heat-sinking layer (i.e., the Ag alloy), which, due to its high thermal conductivity, diffuses the heat rapidly. Consequently, one can safely say that the melt-quenched amorphous mark forms in about one nanosecond.

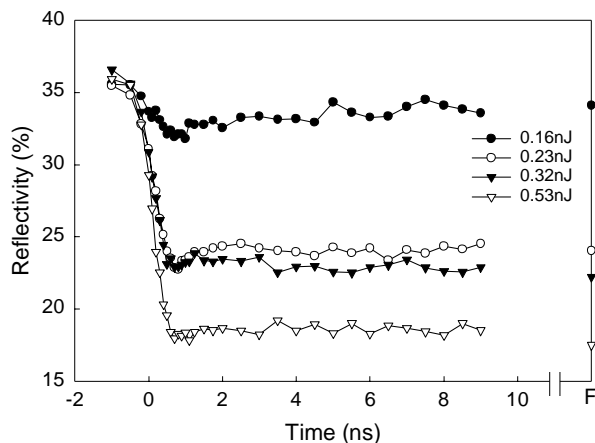


Fig. 3. Reflectivity variations during amorphization of the crystalline state of Bi-doped pseudo-binary GeSbTe film (Disc A). Each curve corresponds to a specific value of the pulse energy. All the pulses have duration of 0.5ns. The right-most point of each curve represents the final reflectivity of the recorded mark (after several minutes).

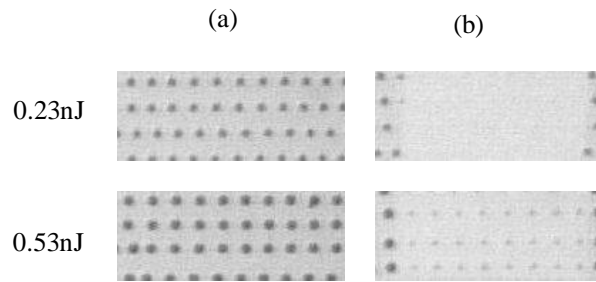


Fig. 4. (a) Optical microscope images of amorphous marks written on a crystalline GSTB film (Disc A). (b) The marks in the central region of the imaged frames were erased by a focused CW laser beam. (Mark spacing = 2.5  $\mu$ m in the horizontal direction.)

Besides the formation of melt-quenched amorphous marks, it is interesting to note that a permanent hole is also formed in the time interval of one nanosecond. We expect this hole to be within the recording layer, and not a through hole (i.e., all the way to the plastic substrate), as there is not enough energy in the pulse to melt the fairly thick metal layer.

#### 4. EXPERIMENTS ON AS-DEPOSITED AMORPHOUS FILM

##### 4.1 Disc A (10-nm lower dielectric layer)

Figure 5 shows reflectivity traces obtained during laser irradiation of the as-deposited GSTB film of Disc A. The energy content of the pulse is varied from 0.05 nJ to 0.40 nJ. The as-deposited region can be crystallized by keeping its temperature long enough between the glass transition temperature  $T_g$  and melting temperature  $T_m$ .<sup>16,17</sup> Investigation of the final reflectivities in Fig. 5 reveals that none of the curves corresponds to crystalline mark formation, and inspection under the static tester shows that writing with 0.20-nJ or higher energy pulses produces unerasable marks (i.e., hole opening). Figure 6 shows optical microscope images of the written marks. These "amorphous" marks are seen to have slightly higher reflectivity than the as-deposited amorphous background. It is clear that marks written with 0.31 nJ contain a dark burned-out hole at their center. With careful inspection, one can ever see very small burned-out holes formed during writing by 0.20 nJ pulses.

The inset in Fig. 5 shows a plot of final reflectivity versus pulse energy. Here, reflectivity is a maximum at 0.15 nJ and drops after this point with the increasing pulse energy (due to the formation of burned-out hole formation). The peak reflectivity is comparable to the value measured for the melt-quenched amorphous state of the sample; see Table 1. We could not record polycrystalline marks on this sample even though we decreased the energy of the short

pulse to very low values, e.g., 0.05 nJ, to prevent melting. This, of course, is expected because the GSTB film does not have enough time to generate nucleation sites throughout the illuminated region with these short pulses.

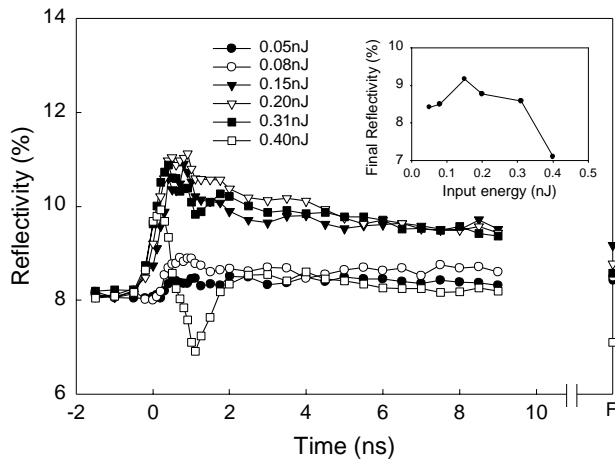


Fig. 5. Reflectivity variations during short-pulse laser irradiation of the as-deposited GSTB film (Disc A). Each curve corresponds to a specific value of pulse energy. All pulses have duration of 0.5 ns. The rightmost data point for each curve represents the final reflectivity after several minutes. The dependence of this final reflectivity on pulse energy is shown in the inset. The background reflectivity of 8.09 % represents the value at zero input energy.

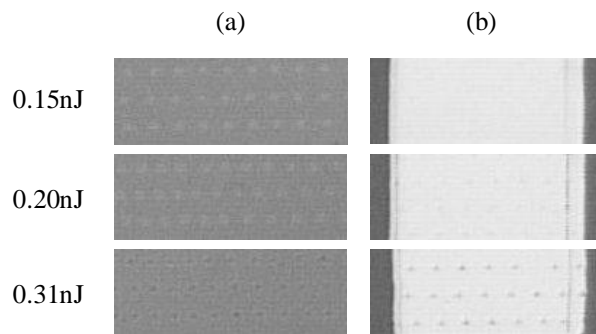


Fig. 6. (a) Optical microscope images of amorphous marks written on the as-deposited amorphous GSTB film (Disc A). (b) The marks in the central region of the imaged frames were erased by a focused CW laser beam. The vertical dark lines in the images of column (b) do not represent burned-out holes during short-pulse writing but burned-out lines during erasing by raster scanning. (Mark spacing = 2.5  $\mu\text{m}$  in the horizontal direction.)

Next, we conducted experiments on the static tester with relatively long pulses on the as-deposited amorphous region of Disc A in order to estimate the approximate onset time of crystallization for this medium. Figure 7 shows reflectivity variations during crystalline mark formation on the as-deposited region of Disc A upon application of a 2.0- $\mu\text{s}$  pulse (pulse duration: 0-2.0  $\mu\text{s}$  in the figure). The reflectivity is normalized by its value for the crystalline state of the sample. The experiments are conducted on a static tester,<sup>11,12</sup> which has two semiconductor lasers operating at  $\lambda_1 = 680$  nm (laser 1) and  $\lambda_2 = 643$  nm (laser 2). We used laser 1 as pump beam for writing and laser 2 as probe beam for reading. A 0.6-NA microscope objective was used to focus both beams onto the same spot at the sample.

This type of transition from the as-deposited amorphous state to the crystalline state is well investigated in the literature.<sup>15,18</sup> In Fig. 7 reflectivity for all the curves starts from its value for the as-deposited state and reaches its final value at around 3-4  $\mu\text{s}$ . Subsequent erasure experiments show that marks written at 16 mW have burned-out holes at the center. We see no indication of mark-formation upon irradiation with 2.0-mW pulses. Otherwise crystalline-marks formed with pulses from 4.0 to 14.0mW, and they were found to be erasable. The difference in the final reflectivity observed for different write powers is caused by differences in the final size of the recorded marks. The highest reflectivity, and consequently the largest mark, was obtained at 12.0 mW write power.

To inspect these transition processes in detail, Fig. 7(b) provides a close-up view of some of the curves in Fig. 7(a). In the time range between 0 and 0.2  $\mu\text{s}$ , we find that the reflectivity takes off right after  $t = 0$ , especially for pulse powers over 4 mW. This is likely caused by the change in the optical constants of the sample with rising temperature.<sup>15,18</sup> Taking this effect into account, the onset time of crystallization can be estimated at around 200 ns, except for the lower two curves (3mW and 2mW), one of which shows a longer onset time and the other may have no crystallization onset at all. The curve corresponding to 14.0 mW of the pulse power shows a lower crystallization rate than that of the 12.0 mW curve, presumably because at higher power the temperature at the center of the beamspot exceeds the melting point; this creates a small amorphous region at the center of the spot depresses the reflectivity.

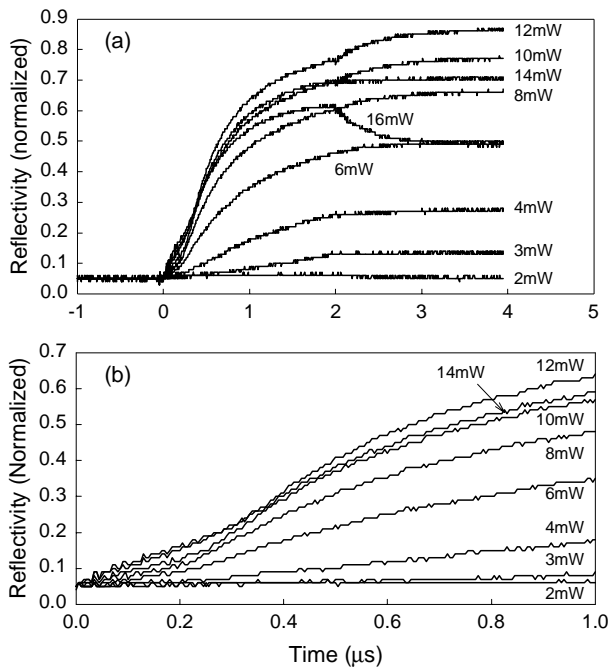


Fig. 7. Reflectivity variations during long-pulse laser irradiation of the as-deposited GSTB film (Disc A). Each curve corresponds to a specific value of the pulse power. All pulses have 2.0- $\mu$ s duration. Reflectivity is normalized by its value for the crystalline state of the sample. Each plot is averaged over 20 identical trials at different locations on the sample. A close-up of reflectivity variations is shown in (b).

amorphous film, the final state of the mark in none of these experiments must be crystalline, similar to the results obtained for Disc A. The marks written with 0.20 nJ or more were found to contain a permanent burned-out region in them after erasure on the static tester. This energy threshold is nearly the same as that for Disc A, despite their differing lower dielectric layer thickness, though the thicker dielectric layer should give Disc B a relatively slow cooling rate and correspondingly low threshold-energy for burn-out. Using heat diffusion arguments, we can understand this phenomenon as follows. Within 0.5 ns, the heat applied to the GSTB film does not have enough time to diffuse to the heat-sinking layer, because the combined thickness of the lower dielectric layer and the GSTB film is larger than the diffusion length on this time scale. Thus all the energy input to the medium is absorbed in the GSTB film during the pulse, irrespective of the thickness of the lower dielectric layer. Therefore, simply determined by the input energy, the threshold of permanent burned-out is the same for Discs A and B.

The inset of Fig. 8 shows the final reflectivities obtained a few minutes after pulse irradiation. The final reflectivity goes up ever so slightly as the energy per pulse increases at first. This is caused by the formation of melt-quenched amorphous marks that have slightly higher reflectivity than the as-deposited film; see Table 1. We inspected the written marks under an optical microscope and observed that the marks written with 0.20 - 0.27 nJ have a burned-out hole surrounded by a melt-quenched amorphous ring. Therefore, at 0.20 nJ the reflectivity increase appears to slow down with the creation of dark, burned-out holes. However, the increase in the area of the melt-quenched amorphous ring surrounding the hole keeps the reflectivity on a rising path. The final reflectivity obtained with a 0.33 nJ pulse shows by far the lowest value in Fig. 8. For the marks written with 0.33 nJ, we find a structure different from those written at lower energy. The marks have a dark annular region surrounding a bright spot in the center. This is probably caused by a permanent structural change in the reflective metal layer as well as in the GSTB layer, whereas the previously noted burned-outs at lower energies are structural changes in the GSTB film alone.

Looking back at Fig. 5, the pulse duration of 0.5 ns turns out to be too short for this film to enable crystallization of the as-deposited amorphous state. It is thus possible, using 0.5-ns laser pulses, to form melt-quenched amorphous marks without forming crystalline rings around them. Thus, the melt-quenched area formed by an array of closely spaced melt-quenched marks discussed in section 2 (in conjunction with Table 1) should be a pure melt-quenched amorphous state without any recrystallized areas.

The results of crystalline-to-amorphous and amorphous-to-crystalline transition discussed so far lead to the following conclusion: even though a phase-change medium may exhibit amorphous-to-crystalline transition in hundred-nanosecond or longer time frames, it can nevertheless form melt-quenched amorphous marks in one nanosecond or less, induced by a sub-nanosecond laser pulse.

#### 4.2 Disc B (20-nm lower dielectric layer)

Figure 8 shows measured reflectivity variations as a result of a 0.5-ns pulse irradiation on the as-deposited region of the GSTB film of Disc B. Experimental conditions for this measurement were the same as those used in our previous experiments on Disc A (Fig. 5). The energy per pulse is varied from 0.08 nJ to 0.33 nJ.

The minimum reflectivity is attained at around 0.6 or 0.7 ns for all the curves except the one with the energy of 0.33 nJ. This result suggests the formation of a different structure by the 0.33-nJ pulse, which will be discussed later. Considering the final reflectivities, which are comparable to the initial value for the as-deposited

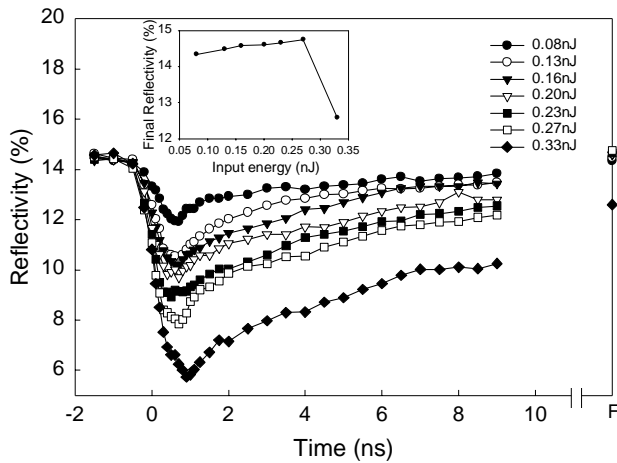


Fig. 8. Reflectivity variations during short-pulse laser irradiation of the as-deposited GSTB film (Disc B). Each curve corresponds to a specific value of the pulse energy. All pulses have 0.5-ns duration. The rightmost point of each curve represents the final reflectivity of the corresponding mark after several minutes. The dependence of this final reflectivity on pulse energy during short-pulse irradiation is shown in the inset. The background reflectivity of 14.51 % represents the value at zero input energy.

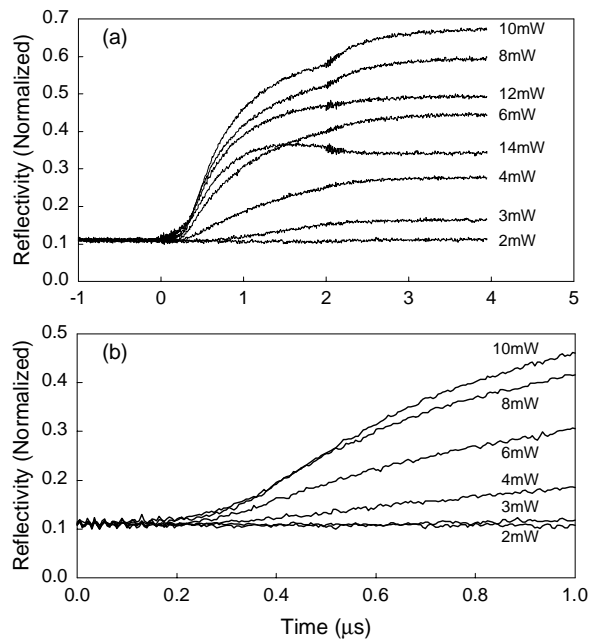


Fig. 9. Reflectivity variations during long-pulse irradiation of the as-deposited GSTB film (Disc B). Each curve corresponds to a specific value of the pulse power. All pulses have 2.0- $\mu$ s duration. Reflectivity is normalized by its value for the crystalline state of the sample. Each plot is averaged over 20 identical trials at different locations on the sample. Close-up of reflectivity variations is shown in (b).

Next, writing experiments on Disc B were performed on a static tester with a 2.0- $\mu$ s rectangular pulse similar to that used for Disc A. Figure 9 shows reflectivity variations upon irradiation of the as-deposited area of Disc B. With 12.0 mW and 14.0 mW, marks are found to have burned-out holes, whereas marks formed with lower powers could be fully erased on the static tester. The curves in Fig. 9 share similar characteristics with those of Fig. 7, which was obtained for Disc A. Focusing on the differences between the results with Disc A and Disc B, we find the threshold power for burn-out to be lower for Disc B, unlike the short-pulse experiment. This is not surprising, considering that heat diffusion now occurs over time intervals much shorter than the pulse duration of 2.0  $\mu$ s. The different thicknesses of the lower dielectric layer thus matter under long-pulse irradiation. Disc A, having a thin upper layer, cools faster during the pulse, thus pushing the threshold power higher than that for Disc B.

Finally, the close-up view of the reflectivity curves of Fig.9 (a), shown in Fig. 9(b), indicates that for Disc B reflectivities do not rise significantly until around 200 ns. Apparently, the change in the optical constants of this sample with rising temperature does not cause much change in the reflectivity of the stack. It is thus easier to determine the onset time of crystallization for the GSTB film of Disc B than it was for Disc A. These should coincide, as the two discs have identical GSTB films, and not surprisingly, we find the same value for the onset time of crystallization, namely, ~ 200 ns.

#### 4.3 Discussion on the change of reflectivity with rising temperature

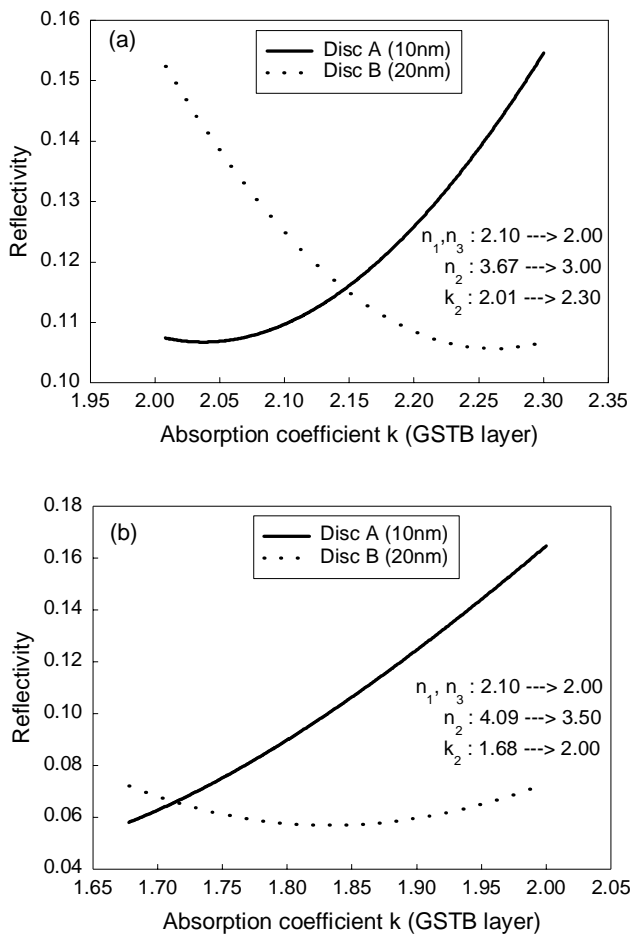


Fig. 10. Calculated reflectivity variations of Disc A and Disc B during heating ((a):  $\lambda = 532$  nm, (b):  $\lambda = 643$  nm). The temperature dependences of the optical constants of each layer are listed in Table 2. All the parameters are changed simultaneously, though only the absorption coefficient  $k$  of the GSTB layer is shown in the horizontal axis.

Comparing the results of Fig. 5 (Disc A) and Fig. 8 (Disc B), we notice a basic difference in the curves. Unlike the results for Disc A, every curve in Fig. 8 goes down in reflectivity upon irradiation by the pulse. This may be due to the change of optical constants with temperature combined with the effect of coherent optical interference between various layers of each disc. Figure 10 shows the calculated reflectivity variations of the two discs during heating. The results for the wavelength of 532 nm are shown in Fig. 10 (a). The optical constants used for both discs are shown in Table 2. The refractive indices of the dielectric layer and the phase-change recording layer are believed to decrease with rising temperature, whereas the absorption coefficient of the phase-change film is expected to increase with rising temperature. Thus we changed the constants as shown in Table 2 for calculating the reflectivity variations of our media. We did not change the indices of the metal reflective layer because it should not be heated much comparing to the other layers. In the Fig. 10 all of the varied parameters are changed simultaneously, although the x-axis of the figure shows only the absorption coefficient  $k$  of the GSTB layer. The change of the optical constants of Disc A favor an increase in reflectivity whereas for Disc B they result in a decrease in reflectivity, which agrees well with the experimental results shown in Fig. 5 and Fig. 8. Even though the two discs differ only in the thickness of the lower dielectric layer (by 10 nm), this difference appears to be sufficient to cause the observed changes in reflectivity upon multiple reflections within the multi-layer stack.<sup>17</sup>

Figure 10 (b) shows the calculated reflectivity variation for  $\lambda = 643$  nm in order to simulate the results obtained on the static tester. The optical constants for this calculation are also shown in Table 2. The changing the optical constants of Disc A caused an increase in reflectivity with rising temperature, whereas for Disc B they resulted in only a slight change. This again agrees well with the experimental results shown earlier in Fig. 7 and Fig. 9.

Table 2. Optical constants of the quadric-layer stacks at room temperature and at an elevated temperature.

	layer	Refractive index (n)	Absorption coefficient (k)	n (heated)	k (heated)
$\lambda = 532$ nm	ZnS-SiO <sub>2</sub>	2.099	0.052	2.000	0.052
	GeSbTeBi	3.672	2.008	3.000	2.300
	Ag alloy	0.120	3.330	--	--
$\lambda = 643$ nm	ZnS-SiO <sub>2</sub>	2.099	0.040	2.000	0.040
	GeSbTeBi	4.092	1.678	3.500	2.000
	Ag alloy	0.128	4.281	--	--

## 5. CONCLUSION

Reflectivity variations during phase-transition between amorphous and crystalline states of two quadrilayer phase-change samples have been investigated with sub-nanosecond laser pulses using a pump-and-probe technique. We created a melt-quenched amorphous mark on the pre-crystallized area of a Bi-doped GeTe-Sb<sub>2</sub>Te<sub>3</sub> pseudo-binary phase-change sample with a 0.5-ns laser pulse. This crystalline-to-amorphous transition was found to complete its course within about one nanosecond. Crystalline formation on the as-deposited amorphous state of this medium did not start upon application of a 0.5-ns pulse, but required at least 200 nanoseconds under a 2.0- $\mu$ s laser pulse irradiation. Simple arguments based on heat diffusion were used to explain qualitatively the time scale of amorphization and the threshold energy for creation of burned-out holes within the phase-change film.

## REFERENCES

1. J. Feinleib, J. deNeufville, S.C. Moss, and S. R. Ovshinsky, "Rapid reversible light-induced crystallization of amorphous semiconductors," *Appl. Phys. Lett.* **18**, 254-257 (1971).
2. R. J. von Gutfeld, and P. Chaudhari, "Laser writing and erasing on chalcogenide films," *J. Appl. Phys.* **43**, 4688-4693 (1972).
3. D. J. Gravestijn, "Materials developments for write-once and erasable phase-change optical recording," *Appl. Opt.* **27**, 736-738 (1988).
4. H. Minemura, H. Andoh, N. Tsuboi, Y. Maeda, and Y. Sato, "Three-dimensional analysis of overwriteable phase-change optical disks," *J. Appl. Phys.* **67**, 2731-2735 (1990).
5. Y. Maeda, I. Ikuta, H. Andoh, and Y. Sato, "Single-Beam Overwrite with a New Erase Mode of In<sub>3</sub>SbTe<sub>2</sub> Phase-Change Optical Disks," *Jpn. J. Appl. Phys.* **31**, 451-455 (1992).
6. C. N. Afonso, J. Solis, F. Catalina, and C. Kalpouzos, "Ultrafast reversible phase change in GeSb films for erasable optical storage," *Appl. Phys. Lett.* **60**, 3123-3125 (1992).
7. J. Siegel, C. N. Afonso, and J. Solis, "Dynamics of ultrafast reversible phase transitions in GeSb films triggered by picosecond laser pulses," *Appl. Phys. Lett.* **75**, 3102-3104 (1999).
8. C. Peng, J. K. Erwin, M. Mansuripur, "Amorphization induced by sub-nanosecond laser pulses in phase-change optical recording media," submitted to *Applied Optics*, (2003).
9. K. Watabe, P. Polynkin, and M. Mansuripur are preparing a manuscript to be called "Optical Pump-and-Probe Test System for Thermal Characterization of Phase Transitions in Thin Films."
10. K. Yusu, S. Ashida, N. Nakamura, N. Oomachi, N. Morishita, A. Ogawa, and K. Ichihara, "Advanced Phase Change Media for Blue Laser Recording of 18 GB Capacity for 0.65 Numerical Aperture and 30 GB Capacity for 0.85 Numerical Aperture," *Jpn. J. Appl. Phys.* **42**, 858-862 (2003).
11. M. Mansuripur, J. K. Erwin, W. Bletscher, P. K. Khulbe, K. Sadeghi, X. Xun, A. Gupta, and S. B. Mendes, "Static tester for characterization of phase-change, dye-polymer, and magneto-optical media for optical data storage," *Appl. Opt.* **38**, 7095-7104 (1999).
12. M. Mansuripur, P. K. Khulbe, X. Xun, J. K. Erwin and W. Bletscher, "Real-time studies of mark formation processes in phase-change and magneto-optical media using a two-laser tester," *J. Magn. Soc. Japan*, **25**, 399-407 (2001).
13. J. H. Coombs, A. P. J. M. Jongenelis, W. van Es-Spiekman, and B. A. J. Jacobs, "Laser-induced crystallization phenomena in GeTe-based alloys. I. Characterization of nucleation and growth," *J. Appl. Phys.* **78**, 4906-4913 (1995).
14. P. K. Khulbe, T. Hurst, M. Horie, and M. Mansuripur, "Crystallization behavior of Ge-doped eutectic Sb<sub>70</sub>Te<sub>30</sub> films in optical disks," *Appl. Opt.* **41**, 6220-6229 (2002).
15. P. K. Khulbe, E. M. Wright, and M. Mansuripur, "Crystallization behavior of as-deposited, melt quenched, and primed amorphous states of Ge<sub>2</sub>Sb<sub>2.3</sub>Te<sub>5</sub> films," *J. Appl. Phys.* **88**, 3926-3933 (2000).
16. E. M. Wright, P. K. Khulbe, and M. Mansuripur, "Dynamic theory of crystallization in Ge<sub>2</sub>Sb<sub>2.3</sub>Te<sub>5</sub> phase-change optical recording media," *Appl. Opt.* **39**, 6695-6701 (2000).
17. A. B. Marchant, *Optical Recording*. (Addison-Wesley, 1990).
18. P. K. Khulbe, X. Xun, and M. Mansuripur, "Crystallization and amorphization studies of a Ge<sub>2</sub>Sb<sub>2.3</sub>Te<sub>5</sub> thin-film sample under pulsed laser irradiation," *Appl. Opt.* **39**, 2359-2366 (2000).